Arab Gulf J. scient. Res. **3** (2), pp. 791-805 (1985)

Performance of Numerical Relative Orientation for Complete and Incomplete Flat Models

Mohamed Shawki Elghazali and Safaa Eldin Moustafa

Department of Civil Engineering, Cairo University, Cairo, Egypt

ABSTRACT. Numerical Relative Orientation using elements of one projector (dependent orientation) has been applied to several cases of complete as well as incomplete stereoscopic models of flat terrain. Parallax observations were made on the Zeiss Jena Stereometrograph E, using the (b_y) screw. Since in all cases more than five observations were available, a least squares solution was used to solve for the five elements of relative orientation. This allowed the accuracy assessment to be based on analysis of variances and covariances. In complete models, the accuracy of the solution improved by increasing the number of the orientation points. However, some elements improved more significantly than others. For incomplete models, the distribution of the orientation points proved to be more significant than their number. The larger the determinant of the coefficient matrix of normal equations, the better was the solution. Ill-conditioned systems resulted in large variances despite an increased number of orientation points.

1. Introduction

Relative orientation may be defined as the process of eliminating y-parallaxes in the overlapping area between two photographs, thus bringing corresponding rays to intersect at model points. Practically, this is equivalent to bringing the two projectors of the stereoscopic plotter in a relative position similar to that of the camera positions during taking the photography. The relative orientation of a model may be achieved by changing the necessary elements of one projector only, while the other projector is left undisturbed (dependent orientation). It may also be achieved by changing the necessary elements on both projectors (independent orientation). The former method is useful in the bridging method of aerial triangulation where one projector has to be kept fixed during strip formation. This method has been used in this research in which the five elements of one projector are determined numerically.

In numerical relative orientation, the changes to be given to the elements are computed from the parallax equations with the help of parallax measurements. This method has the advantage of eliminating the subjectivity usually associated with empirical methods due to human judgement in eliminating y-parallaxes. Accordingly, in jobs involving several models as in the case of aeropolygon or independent model triangulation blocks, it is possible to use more than one operator on different shifts while maintaining the homogeneity of the observations. This feature is certainly attractive from a managerial point of view. However, the main advantage of numerical relative orientation is that it allows by using more than five parallax measurements, – provided that their geometry is non singular – the computation of relative orientation elements based on a least squares adjustment. The result would be best linear unbiased estimates of the elements (X), together with their variance – covariance matrix (Σ_X) enabling us to assess the quality of the solution. This is rather significant particularly in incomplete models since the distribution of the orientation points has a direct effect on the accuracy of different elements.

2. Mathematical Model

The relation between the differential Y shift (dY) in the model space in a plane of constant (Z) due to translations Δbx, $\Delta$by, Δbz together with rotations $\Delta\omega$, $\Delta\phi$, $\Delta\varkappa$ of a projector is given by equation (1), Ghosh (1972).

$$\mathrm{dY} = \Delta \mathrm{by} - \frac{\mathrm{Y}}{\mathrm{Z}}\Delta \mathrm{bz} - \mathrm{Z}\left(1 + \frac{\mathrm{Y}^2}{\mathrm{Z}^2}\right)\Delta\omega - \left(\mathrm{X}\sin\omega - \frac{\mathrm{XY}}{\mathrm{Z}}\cos\omega\right)\Delta\phi$$
$$+ \left(\mathrm{X}\cos\phi\cos\omega - \mathrm{Z}\sin\phi - \frac{\mathrm{XY}}{\mathrm{Z}}\cos\phi\sin\omega - \frac{\mathrm{Y}^2}{\mathrm{Z}}\sin\phi\right)\Delta\varkappa \tag{1}$$

where

dY is the shift of a point in the Y direction
X, Y, Z are the model coordinates of the point
$\Delta$by, Δbz are differential movements of projector in Y & Z directions
$\Delta\omega$, $\Delta\phi$, $\Delta\varkappa$ are differential rotations of projector around X, Y, Z axes
ω, ϕ, $\varkappa$ are angles of rotation around X, Y, Z axis
For full details concerning derivation of equation (1) see Ghosh (1972), Zeller (1952) or Brandenberger (1947).

In vertical or near vertical photography, it is common to assume $\omega = \phi = 0$. Accordingly, equation (2) results after substituting a zero value for ω and ϕ.

$$\mathrm{dY} = \Delta \mathrm{by} - \frac{\mathrm{Y}}{\mathrm{Z}}\Delta \mathrm{bz} - \frac{\mathrm{Z}^2 + \mathrm{Y}^2}{\mathrm{Z}}\Delta\omega + \frac{\mathrm{XY}}{\mathrm{Z}}\Delta\phi + \mathrm{X}\Delta\varkappa \tag{2}$$

If we denote the initial parallax at point (i) by (P_{y_i}), then relative orientation changes should be introduced, such that the parallax is eliminated at point (i) by introducing a change ΔP_{y_i}. Accordingly,

$$P_{y_i} + \Delta P_{y_i} = 0$$

or

$$\Delta P_{y_i} = -P_{y_i} \tag{3}$$

Generally, movements introduced to both projectors I and II result in differential Y shifts dY_I and dY_{II} respectively. Accordingly, ΔP_{y_i} can be expressed as the difference between differential shifts of both projectors, or more generally:

$$\left.\begin{aligned}
&\Delta P_y = (dY_I - dY_{II}) = -Py = \\
&\Delta by_I - \frac{Y}{Z}\Delta bz_I - \frac{Z^2 + Y^2}{Z}\Delta\omega_I + \frac{XY}{Z}\Delta\phi_I + X\Delta\varkappa_I \\
&-\Delta by_{II} + \frac{Y}{Z}\Delta bz_{II} + \frac{Z^2 + Y^2}{Z}\Delta\omega_{II} - \frac{(X-b)Y}{Z}\Delta\phi_{II} - (X-b)\Delta\varkappa_{II}
\end{aligned}\right\} \tag{4}$$

where b is the base representing the distance between the left and right projection centers, Fig. 1. Equation (4) represents the fundamental formula for relative orientation. In this equation only five coefficients are linearly independent, therefore only five of the ten unknowns can be determined. These are the five parameters of the relative orientation. Regrouping with respect to the independent coefficients of equation (4), we arrive at the orientation formula with pseudo-unknowns.

$$\Delta Py = -P_y = \frac{XY}{Z}\Delta A - \frac{Z^2 + Y^2}{Z}\Delta B - \frac{Y}{Z}\Delta C + X.\Delta D + \Delta E \tag{5}$$

where

$$\begin{aligned}
\Delta A &= \Delta\phi_I - \Delta\phi_{II} \\
\Delta B &= \Delta\omega_I - \Delta\omega_{II} \\
\Delta C &= \Delta bz_I - \Delta bz_{II} - b\Delta\phi_{II} \\
\Delta D &= \Delta\varkappa_I - \Delta\varkappa_{II} \\
\Delta E &= \Delta by_I - \Delta by_{II} + b\Delta\varkappa_{II}
\end{aligned}$$

Since the dependent method of relative orientation using projector (II) is employed, the final equation for numerical relative orientation is given by (6).

$$-P_y = -\Delta by_{II} + \frac{Y}{Z}\Delta bz_{II} + \frac{Z^2 + Y^2}{Z}\Delta\omega_{II} - \frac{(X-b)Y}{Z}\Delta\phi_{II} - (X-b)\Delta\varkappa_{II} \tag{6}$$

Equation (6) is obtained from equation (4) after substituting zero values for the elements of projector (I), since it is kept unchanged during the orientation process.

3. Experiment Set-up

3.1. Parallax Measurements

Numerical relative orientation is based on parallax measurements at five or more points in the model space arranged in such a way that they do not conform to critical or singular geometry. If parallaxes are measured at only five points, then use of equation (6) results in a unique solution for the unknowns. By using parallax observations at more than five points, a solution based on a least squares algorithm is utilized. Points (1, 2, 3, 4, 5 & 6) are always referred to as the six standard points. Y-Parallaxes can be measured either by using the (b_y) control knob or the (ω) control knob of the stereoscopic plotter. However, since the effect of ω rotation is non-linear then the left hand side of equation (6) should be simply modified to account for this non-linearity of the movement, according to equation (7).

$$\omega_y\left(\frac{Z^2 + Y^2}{Z}\right) = -P_y \qquad (7)$$

In this research, the b_y screw was used to measure the Y-parallaxes and accordingly equation (6) was employed. Stereoscopic models were set on the Zeiss (Jena) stereometrograph E after proper calibration and adjustment of the stereoplotter. Inner orientation was first performed followed by a coarse empirical relative orientation. Then Y-parallaxes were measured for twelve points symmetrically distributed within the model area, Fig. 1.

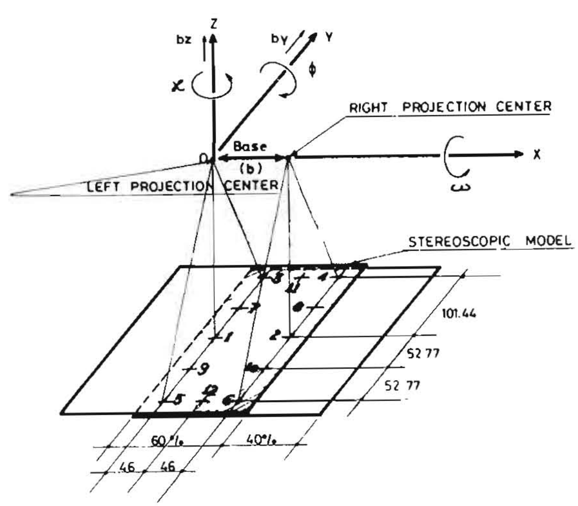

Fig. 1. Coordinate system, model dimensions and locations of orientation points (Dimensions in mm)

3.2. Repeated Parallax Observations

There is a false concept that repeating parallax observations will contribute to the accuracy of the solution. This is not true as we will illustrate next. The variances of Y-parallaxes (σ_R^2) depend upon the geometric exactness of the two photographs (σ_P^2), the instrumental errors (σ_I^2) and the extent of elimination of the parallax, *i.e.* the observation (σ_0^2). Assuming no correlation among different groups of errors, the relation between these variances can be expressed according to (8).

$$\sigma_R^2 = \sigma_P^2 + \sigma_I^2 + \sigma_0^2 \tag{8}$$

Experience has shown that typical estimates for these variances would be $\sigma_P^2 = 25\mu^2$, $\sigma_I^2 = 50\mu^2$ using analog instruments and $\sigma_0^2 = 25\mu^2$, Hoschtitzky (1970). Accordingly, substituting these values in equation (8) will result in a value of $\sigma_R = 10\mu$. Repeated parallax observations at one model point will improve the precision very slightly, as σ_p and σ_I will behave systematically. For repeated (n) observations, the mean variance of Y-parallax (σ_{MR}^2) may be then expressed by (9).

$$\sigma_{MR}^2 = \sigma_P^2 + \sigma_I^2 + \frac{\sigma_o^2}{n} \tag{9}$$

Equation (9) is represented graphically in Fig. 2 from which we see that as (n) approaches (∞), σ_{MR} drops from 10μ to approximately 8.6μ. Therefore, more than two cycles of parallax observations can not be economically justified. In fact the main reason for repeating parallax observations is checking against blunders rather than improving the precision. Parallax measurements for the twelve points of Fig. 1 were observed two times for each point using the b_y screw, then taking their arithmetic mean.

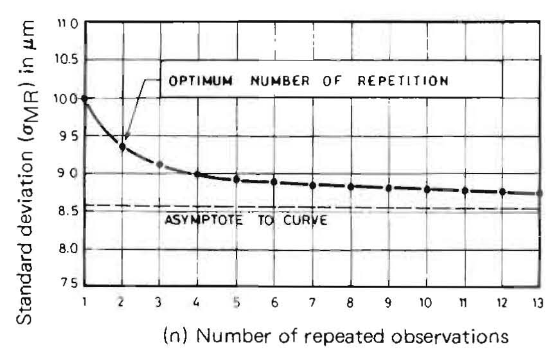

Fig. 2. ($\sigma_{\text{Mean Parallax}}$) Versus repeated observations

3.3. Cases of Study

To test the performance of the procedure of numerical relative orientation for flat terrain for complete and incomplete models, eleven different configurations have been studied, Fig. 3. For complete models, the objective was to test the accuracy of the solution by increasing the number of relative orientation points. Six different point configurations have been tested using 7, 8, 9, 10, 11 & 12 points as shown in Fig. 3a.

Due to the existence of large bodies of water or clouds, especially along the coastal zones, the problem of incomplete models arise. In these models, a portion of the stereoscopic model is lost, thus resulting in poor geometry. Five different cases have been investigated as shown in Fig. 3b.

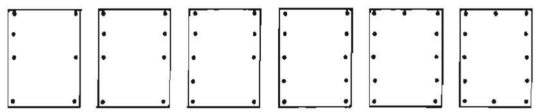

Fig. 3a. Configuration of orientation points (Complete models)

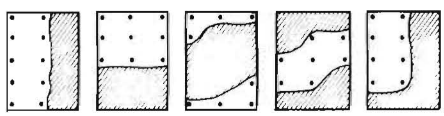

Fig. 3b. Configuration of orientation points (Incomplete models)

In all cases of complete and incomplete models, accuracy assessment was based on testing the variance-covariance matrix of unknown paramaters, correlation coefficients and geometry of orientation points.

3.4. Weighing Scheme

A proper solution using a least squares algorithm requires adequate estimates for weights of observations. In trying to find the correct approach to this problem, we observe that the weight of an individual parallax observation depends apart from the operator's personal capability on the following factors, Ghosh (1963):

A. The attitude of intersections of individual rays at point of intersection.
B. Obliquity of the epipolar plane through the point of intersection.
C. Change in the scale of detail.
D. Different photographic resolution.

Table 1 Weights according to different factors

Points	Weight due to factor				Final average Weight
	A	B	C	D	
1	1	1	1	1	1
2	1	1	1	1	1
3	0.55	0.83	1	0.27	0.66
4	0.55	0.83	1	0.27	0.66
5	0.55	0.83	1	0.27	0.66
6	0.55	0.83	1	0.27	0.66
7	0.85	0.95	1	0.18	0.75
8	0.85	0.95	1	0.18	0.75
9	0.85	0.95	1	0.18	0.75
10	0.85	0.95	1	0.18	0.75
11	0.64	0.83	1	0	0.62
12	0.64	0.83	1	0	0.62

These factors are analysed to finally formulate the weights due to each as well as their joint effect. Summary of the weighing scheme is given in Table 1. For more details concerning the derivation of these weights see Ghosh (1963) and Moustafa (1983).

These weights represent the statistical properties of the observations which is referred to as the *stochastic model*. This model designates the nondeterministic (probabilistic) properties of the observations, whereas the *functional model* as expressed by eqn. (6), for example, describes the deterministic properties of the physical situation under consideration. Both functional and stochastic models constitute the *mathematical model*.

4. Results and Analysis

For each case of complete and incomplete model, the observation and normal equations were formed and the solution of the relative orientation parameters obtained. A program in BASIC language for the 'Hewlett-Packard system 45' version was developed according to the following steps,

$$_{n}[R]_{1} + {}_{n}[A]_{5} \cdot {}_{5}[X]_{1} = {}_{n}[\bar{O}]_{1} \tag{10}$$

$$\underbrace{[A]^{T} \cdot [P] \cdot [R]}_{u} + \underbrace{[A]^{T} \cdot [P] \cdot [A]}_{N} \cdot [X] = [0] \tag{11}$$

or more concisely

$$ {}_{5}[N]_{5\,5}[X]_{1} + {}_{5}[U]_{1} = {}_{5}[\bar{O}]_{1} \tag{12} $$

Then the solution is obtained as follows,

$$ [X] = -[N]^{-1} \cdot [U] \tag{13} $$

where

[R] is the vector of parallax observations
[A] is the coefficient matrix of observations
[X] is the vector of unknown parameters
[P] is the weight matrix of observations

Following the solution of each case, the observational residuals V are obtained from which the following statistical measures are determined.

$$ \hat{\sigma}_0^2 = [V]^T \cdot [P] \cdot [V]/DF \tag{14} $$

$$ \Sigma_x = \hat{\sigma}_0^2 \cdot [N]^{-1} \tag{15} $$

$$ \Sigma_{obs} = \hat{\sigma}_0^2 \cdot [A] \cdot [N]^{-1} \cdot [A]^T \tag{16} $$

where
$\hat{\sigma}_0^2$ is the a posteriori variance of unit weight
DF is the degrees of freedom
Σ_x is the variance covariance matrix of unknowns
Σ_{obs} is the variance covariance matrix of observations

Finally, the correlation coefficients (r_{xy}) between any two variables x & y are computed for the elements of relative orientation (eqn. 17).

$$ r_{xy} = \frac{\sigma_{xy}}{\sigma_x \sigma_y} \tag{17} $$

4.1. Cases of Complete Models

Figure 4, shows the improvement in the solution of the rotational elements of the relative orientation by increasing the number of orientation points. Using twelve symmetrically distributed points instead of seven improved σ_ω & $\sigma_\varkappa$ by 20% whereas σ_ϕ improved by approximately 12%. This is because the ϕ movement has its maximum effect only at the four corner points of the model. It can be also noticed that by using points 11 and 12 the accuracy of ω improved significantly while accuracy of ϕ and $\varkappa$ increased slightly. This is explained by the fact that the y-component of ϕ and $\varkappa$ movement is nil at points 11 and 12. Meanwhile ω movement will have its y-component at points 11 and 12 of the same magnitude as the four corner points 3, 4, 5 & 6. Accordingly σ_ω dropped clearly by adding points

11 and 12 to the orientation points. In fact, the ω-solution may be obtained separately using parallax measurements at three points located on a cross-section whose X coordinates are similar, provided that the determinant of the coefficient matrix is non-singular, *i.e.*,

$$\det\left[\frac{Z^2+Y^2}{Z}\ ;\ \frac{Y}{Z}\ ;\ -1\right] \neq 0$$

The relation between the number of orientation points and the standard deviations of Δb_y and Δb_z elements is shown in Fig. 5 and 6, respectively. It is clear that the improvement in Δb_y was nearly linear and increased by 20% when the number of points increased from seven to twelve. The linear behaviour agrees with the theoretical expectation since Δb_y element has a uniform effect over the whole model area, independent of the location of the points. The small deviations from

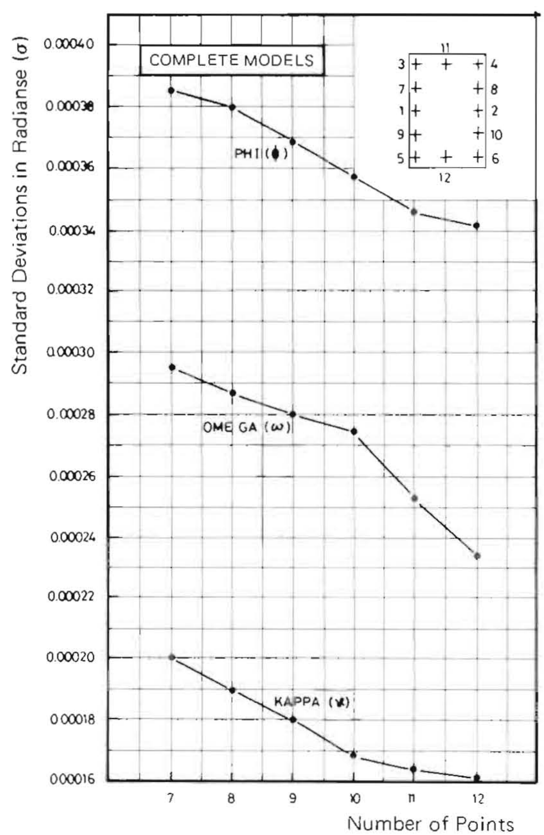

Fig. 4. Standard deviations of rotational elements (ω,ϕ,$\varkappa$) against number of orientation points

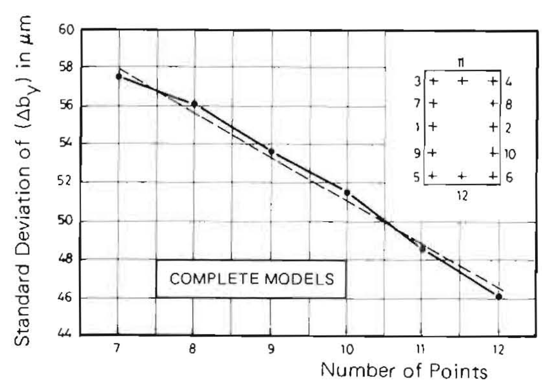

Fig. 5. Improvement of (σ Δb_y) versus orientation points

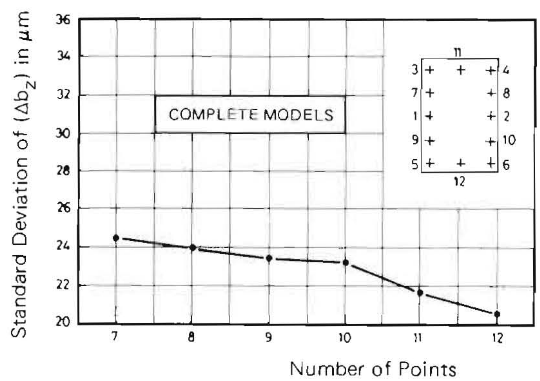

Fig. 6. Improvement of (σ Δb_z) versus orientation points

the straight line (dotted line) is attributed to the stochastic noise associated with the parallax observations. The standard deviation of Δb_z element improved by approximately 16% when using 12 instead of 7 points. Meanwhile, points # 11 and 12 were more significant because of the same previously mentioned reason for the ω element.

Table 2 gives a summary of the standard deviations of the five elements of relative orientation for the different cases of complete models together with the a posteriori variance of unit weight ($\hat{\sigma}_0^2$).

Table 2 Accuracies from cases of complete models

σ Elements \ # Points	7	8	9	10	11	12
$\sigma_\varphi \cdot (10)^3$ rad	0.385	0.379	0.368	0.357	0.346	0.341
$\sigma_\omega \cdot (10)^3$ rad	0.295	0.287	0.280	0.274	0.252	0.234
$\sigma_\varkappa \cdot (10)^3$ rad	0.202	0.189	0.179	0.168	0.163	0.160
$\sigma \Delta b_z \cdot (10)$ mm	0.245	0.240	0.235	0.233	0.218	0.206
$\sigma \Delta b_y \cdot (10)$ mm	0.577	0.562	0.542	0.521	0.489	0.461
$(\hat{\sigma}_0^2)$	0.943	0.963	0.969	0.976	0.918	0.889

4.2. Cases of Incomplete Models

Incomplete models exist due to clouds or water bodies, thus causing serious problems to the operators in performing empirical relative orientation. The practice of taking elevations or measurements of the water level on shores, in addition to available orientation points, becomes generally a procedure with many iterations and, therefore, rather time consuming. However, the use of the x-component of ϕ or ω motions, in conjunction with elevation measurements may lead to a better solution, Klaver (1979). In these cases, the use of numerical relative orientation

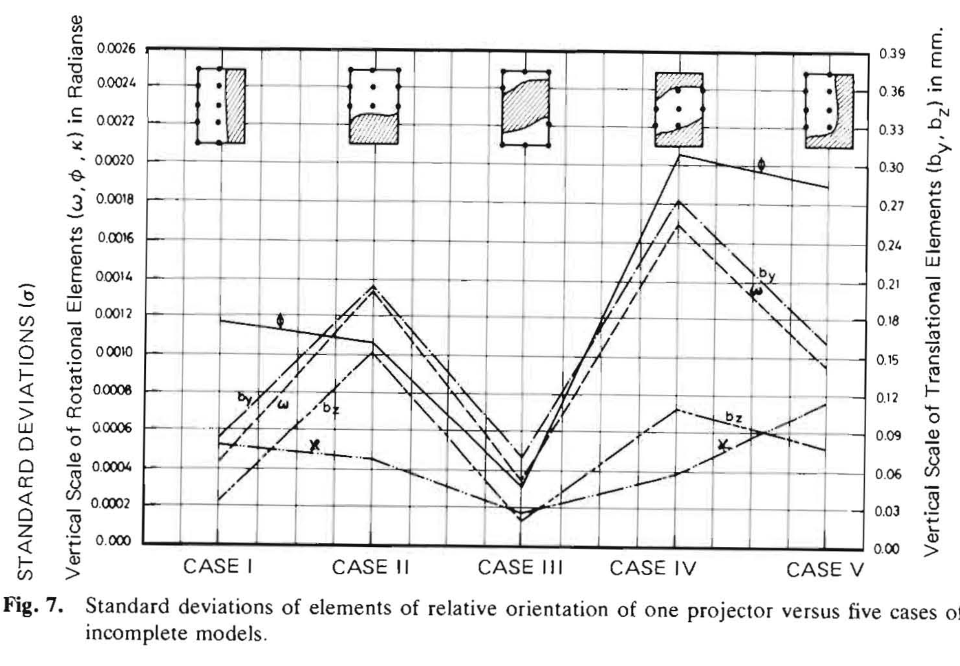

Fig. 7. Standard deviations of elements of relative orientation of one projector versus five cases of incomplete models.

Table 3 Accuracies from cases of incomplete models

Case # / σ Elements	I	II	III	IV	V
$\sigma_{\varphi} \cdot (10)^3$ rad	1.180	1.060	0.328	2.070	1.890
$\sigma_{\omega} \cdot (10)^3$ rad	0.428	1.360	0.339	1.710	0.958
$\sigma_{\varkappa} \cdot (10)^3$ rad	0.527	0.459	0.181	0.398	0.771
$\sigma \Delta b_z \cdot (10)$ mm	0.364	1.528	0.193	1.101	0.785
$\sigma \Delta b_y \cdot (10)$ mm	0.815	2.024	0.716	2.734	1.639
$(\hat{\sigma}_0^2)$	1.175	0.858	0.326	0.807	1.682

procedure becomes a valuable tool, particularly since numerical procedures eliminate the subjectivity of the empirical method caused by the operator's judgement concerning the location of the orientation points or the procedure to be followed. Figure 7, shows the standard deviations for the rotational and translational elements for the five configurations of orientation points of incomplete models used in the study. Results from each of the five cases are analysed separately as follows, whereas all accuracy figures are presented in Table 3.

Case I

This case is known as the case of incomplete models with complete cross-section. In this case, at least one cross-section with x = constant exists somewhere in the model, where three orientation points j, (j + 2), (j + 4) can be chosen such that

$$Y_j = 0; \frac{Y_{j+2}}{Z_{j+2}} = -\frac{Y_{j+4}}{Z_{j+4}} = \text{constant}$$

In this case, the ω solution is nearly as accurate as the case of complete model (σ_ω = 0.00043 radianse). The ϕ solution, on the other hand, deteriorated due to the absence of points # 4 & 6 that are very significant for this element. The other elements remained within tolerances. In this case, ten orientation points were used for the elements determination.

Case II

The upper half of the model is assumed to be clear and nine evenly distributed points were used. Due to the nonexistence of a complete cross-section, the ω solution deteriorated significantly. The $\varkappa$ and ϕ elements improved slightly due to the use of points # 2 and 4. Meanwhile, b_y and b_z deteriorated at almost the same rate as ω.

Case III

Although the obscurèd area of case III is equal or even larger than other cases, this case resulted in the highest accuracy. Accuracy figures shown in Table 3 are comparable to those of complete models. This is simply due to the fact that the distribution of orientation points within the model approaches the case of the six standard models. For all the solved elements, the accuracy was consistently higher than all other cases.

Case IV

Here the distribution of points approaches the case of a singular system, since the orientation points are scattered close to a straight line that connects points 8 and 9. Since the points are not exactly lying on a straight line, the system is known to be ill-conditioned. In mathematical terms, the determinant of the coefficient matrix of the normal equations will be very small. In extreme cases, the coefficient matrix of the normal equation will suffer from a rank deficiency and accordingly its inverse can not be obtained. Such an incomplete model should be rejected for mapping purposes and ground surveying methods should be used instead.

Case V

This case improved the accuracy as compared to the previous case particularly for the (ω) and (b_y) solutions due to the existence of two incomplete cross-sections. However, the results are generally considered poor.

Results from each case of complete as well as incomplete models have been statistically tested. A chi-square (χ^2) test has been used to test the a priori versus the a posteriori variance of unit weight. It has been shown that (DF . $\hat{\sigma}_0^2/\sigma_0^2$) follows a χ^2 distribution. In addition, testing of a posteriori variances between different cases was carried out. It has been also shown that $(\hat{\sigma}_1^2/\hat{\sigma}_2^2)$ follows F-distribution depending on the degrees of freedom of the cases, Hamilton (1964). For complete details concerning such testing see Moustafa (1983).

5. Conclusion

Numerical relative orientation for the complete model cases offers no problem. The accuracy of the elements improved by increasing the number of orientation points. However, the improvement of each element differs depending upon the location of these points within the model space. For incomplete models, the distribution rather than the number of points affects the accuracy directly. The study showed that the accuracy of the solution is a function of the numerical value of the determinant of the coefficient matrix of normal equations (N). The larger the determinant $|N|$, the more accurate will be the solution. Referring to Fig. 7, the computations showed that det $|N|_{III} >$ det $|N|_{I} >$ det $|N|_{II} >$ det $|N|_{V}$ det $|N|_{IV}$.

However, individual elements may be improved by careful choice of point location. Imperfections in the relative orientation elements cause model deformation. Linear model deformation in height is completely removed during the absolute orientation phase. Only non-linear errors due to ϕ and ω elements will remain. The covariance $\sigma_{\omega.\phi}$ will be zero, as long as the two orientation points used for the solution of the ϕ and b_z elements have the same y-coordinates. If two pairs of points are used for this purpose, each pair should have the same y-coordinate to keep $\sigma_{\omega.\phi}$ as zero. Finally, it should be pointed out that the advantage of numerical over empirical relative orientation becomes clear in the case of incomplete models. Apart from solving the relative orientation elements in a systematic way, the eventual residual parallaxes are distributed according to the fixed principle of least squares. For this reason, the use of numerical methods are of great significance during phototriangulation when more than one operator works simultaneously in different shifts.

Acknowledgement

The authors would like to thank Prof. Dr. Shaban, Professor of Surveying and Photogrammetry, Cairo University, for his help throughout the research. Thanks are also due to the Survey Department of Egypt for use of their Zeiss Jena Stereometrograph (E).

References

Brandenberger, A. (1947) *Fehlertheorie der Äusseren Orientierung von Steilaufnahmen*, Ph.D. Dissertation, E.T.H., Zürich, pp. 35-68.

Gosh, S. (1963) Determination of Weights of Parallax Observations for Numerical Relative Orientation, Photogrammetric Engineering, September, *J. Am. Soc. Photogram.*, **29**: 1312-1321.

Ghosh, S. (1972) *Theory of Stereophotogrammetry*, Edwards Brothers, Inc., Ann Arbor, Michigan, pp. 16-27.

Hamilton, W. (1964) *Statistics in Physical Science*, The Roland Press Company, New York, pp. 81-94.

Hoschtitzky, H. (1970) *Theory of Relative and Absolute Orientation of near vertical photographs using Analogue Instruments*, Publications of the International Institute for Aerial Survey and Earth Sciences, The Netherlands, pp. 89-93.

Klaver, J. (1979) Incomplete or Water Models-A pain in the Eye?, *45th ASP-ACSM Conference, March, Washington, D.C.*, pp. 233-245.

Moustafa, S. (1983) *Study on the Accuracy of the Solution of Numerical Relative Orientation*, M.Sc. Thesis, Faculty of Engineering, Cairo University, pp. 61-118.

Zeller, M. (1952) *Textbook of Photogrammetry*, Lewis, London, pp. 32-50.

(Received 24/05/1984;
in revised form 16/10/1984)

أداء عملية التوجيه النسبى الحسابية لنماذج الأرض المستوية الكاملة وغير الكاملة

محمد شوقى الغزالى و صفاء الدين مصفى

كلية الهندسة - جامعة القاهرة - مصر

تم تطبيق عملية التوجيه النسبى الحسابية باستخدام عناصر المسقط الواحد على عدة حالات من النماذج المجسَّمة الكاملة والناقصة للأراضى المستوية. وقد أخذت قراءات الابتعاد الرأسى على جهاز التوقيع «زايس ستريومتر وجراف» بواسطة مسمار الحركة الرأسية. وحيث إنه فى جميع الحالات تواجد أكثر من خمسة أرصاد، فقد استخدمت طريقة أقل مجموع مربعات لحل عناصر التوجيه النسبى الخمسة، وبذلك أمكن تقييم الدقة بتحليل الأخطاء والارتباط بينها. وقد وجد أن دقة الحل قد ارتفعت بزيادة عدد نقاط التوجيه فى حالة النماذج الكاملة ولكن بعض العناصر تحسنت بصورة أوضح من غيرها. أما فى حالة النماذج الناقصة، فإن توزيع نقط التوجيه كان أكثر أهمية من عددها. فكلما زادت قيمة محددة مصفوفة المعادلات الأصولية كلما كان الحل أحسن. وفى حالة النظم غير المتينة هندسياً، فإن الأخطاء الناتجة تفوق المسموح به حتى بزيادة عدد نقاط التوجية.